

Nanoemitters in a defect layer embedded in photonic crystals: synthesis and optical characterization

Hong P. N., Guennouni-Assimi Z., Farha R. , Faure M-C., Goldmann M., Marcillac W., Coolen L., Maitre A., Schwob C., Benalloul P.

Abstract. Manipulation of the emission of nanocrystals embedded in photonic crystals can provide single photon source for quantum information.

Artificial opals are 3D photonic crystals whose synthesis is based on self-assembly of dielectric spheres. This cost-efficient and versatile method does not require a high technological platform and leads to nanostructured samples over cm range. In order to obtain light confinement inside opals, several fabrication methods have been used to create a defect. Artificial opals with a planar defect can be considered as a good "model system" to study the modification of the optical properties of nanoemitters in a photonic crystal.

We will present two efficient and reliable methods to engineer a defect between two silica opals: by sputtering a controlled amount of silica or by the transfer of a monolayer of silica spheres of different diameter by the Langmuir-Blodgett or Schaefer technique. The optical properties of the prepared samples were characterized by transmission and specular reflection spectra. Tunable and highly transmitted and reflected optical modes were evidenced, in good agreement with Finite Difference Time Domain simulations (FDTD).

Colloidal II-VI nanocrystals are efficient and stable emitters which can emit single photons. These nanoemitters were introduced in the defect. The collected fluorescence of these nanocrystals presents an emission diagram which is modified by the photonic crystal and especially by the defect layer.

Key Words and Phrases: Photonic Crystals, Defect Layer, Photoluminescence, Specular Reflectivity

1. Introduction

Quantum information requires a source of single photons emitted at a very high rate in connection with their short decay time [28]. 3D-photonic crystals can control and manipulate the fluorescence properties of embedded quantum emitters such as their decay time and their propagation direction. Quantum information application as others like low-threshold lasers requires insertion of a controlled defect inside this kind of structure. Indeed this disruption of the photonic crystal periodicity can create permitted optical frequency bands within the band gap: light whose frequency is included in the corresponding pass

band is then localized in the defect allowing effects such as wave guiding and confinement for an enhanced emission.

Photonic crystals (PCs) in the visible and near infra-red ranges are characterized by a periodic dielectric constant at wavelength scale. Many approaches have been proposed to fabricate 3-D periodically modulated dielectric materials. Some of them come from more or less well established microelectronic industry processes such as semiconductor layer-by-layer nanomachining [12], layer-by-layer direct laser writing [33, 9, 22], interference lithography using a single diffraction mask [10], holographic lithography with at least 4 laser beams [8], [21] or two-beam only but with multi-exposure [15]. Alternatively to these methods which have known different sophisticated modifications proposed by several groups, bottom-up techniques taking advantage of the spontaneous self-organisation of spherical colloidal particles have been investigated. Various self-assembly techniques have been studied as they provide a low cost and relatively easy protocol to obtain artificial opals. These cheap and versatile methods do not require a high technological platform and can lead to nanostructured samples over cm range. Well orientated faced centered cubic (fcc) crystals have been formed by gravity [1], [19, 20] or controlled sedimentation onto patterned substrate [7]. Different convective methods such as vertical evaporation [14], induced by a temperature gradient [40] or by isothermal heating evaporation-induced self assembly (IHEISA) at a heating temperature of the solvent very close to its boiling point (method indicated for large balls) [41], have provided large mono-domain opals. Langmuir-Blodgett (LB) technique is a layer-by-layer procedure for the preparation of large area synthetic opals. Solid films of particles are transferred from the water surface onto substrates. The results suggest that a successful synthesis of ordered monolayers of monodisperse silica spheres with the LB technique depends critically on the hydrophilic/hydrophobic balance [34], [29]. Each technique has received large attention and several groups have proposed modifications and improvements.

Silica spheres opals have been the object of a large number of papers even if these opals do not present a complete photonic bandgap due to the low index difference between silica and air. Nevertheless the pseudo photonic band gap, called stop-band, affects the propagation of light through the opal and causes transmission dips or reflectance peaks in the sample spectra depending on the direction.

2. Synthesis of silica spheres and opals

The opals were synthesized from home-made silica spheres. The key point to fabricate high crystallographic quality opals over large monodomains is the low size dispersion of the spheres. These ones were obtained from a "multi-steps" synthesis protocol derived from the Stober method [32] which consists in the hydrolysis and condensation of a silica precursor (tetraethylorthosilicate - TEOS) in alcoholic medium, using ammonia as a catalyst. The precursor is added in several steps in order to first create silica seeds and then make them grow. With this method followed by a centrifugation step to select the particles in size, the obtained dispersion size was of the order of 3 to 5%. The diameter of the spheres was between 250 and 550 nm so that the stop band of the corresponding opals appeared in

the visible part of the spectrum. The procedure is described on Figure 1.

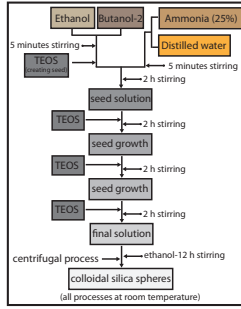


Figure 1: Process Used to Synthesize Silica Spheres.

The opals were synthesized using the convection self-assembly protocol [14] as this procedure gives the best face centered cubic structure (fcc) with the largest monodomains. In the case of direct opals, the photonic band gaps are incomplete: the corresponding stop bands can be evidenced as peaks in the optical reflection spectra [5, 23, 38, 13, 4, 6, 39, 24].

Specular reflection spectra

The opal specular reflection spectra were measured at various incidence angles. The incidence beam was provided by a halogen lamp connected to an optical fiber (core 600 μm), mounted on a goniometer arm with a collimator (focal length 12.7 mm) and a diaphragm (diameter 0.6 mm). The reflected beam was collected by a symmetric collimated fiber (with 1 mm diaphragm) and analyzed by a spectrometer (resolution 1.5 nm). The overall goniometer resolution was 1° . All the spectra were normalized by the incident light spectrum. The stop band shifted to lower wavelengths as the incidence angle increased (Figure 2) [2].

The dependence of the wavelength of the stop band as a function of the considered propagation direction can be treated in two ways. A first way is to calculate numerically the three-dimensional band structure of the opal [17]. A second way is to model the opal by a lattice of scattering points (located at the center of the spheres) in a homogeneous medium with an effective index n_{eff} . At a given incident light angle, the opal stop band wavelength is then provided by the Bragg's law which expresses the condition for constructive interferences between beams reflected by parallel planes of scattering points [5, 23, 3, 30, 35]. The Bragg's law can be considered as a first approximation as the refractive index of silica and air are not too different. The second peak in the specular reflection spectra for incidence angles around 45° takes evidence that the prepared opals have the fcc structure with low defect density [2].

The presence of the stop-band in these photonic crystals is of great interest for nano-emitters fluorescence manipulation. If nano-emitters, whose emission frequency is in the forbidden frequencies band, are embedded in the photonic crystal, their fluorescence will be inhibited in certain directions, leading to modifications of their emission diagram. Moreover, thanks to the Fermi golden rule, the changes in the local density of states (LDOS)

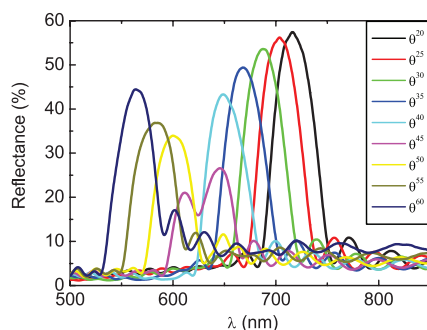


Figure 2: Specular Reflection versus the Incidence Angle.

induced by the photonic crystal will affect their spontaneous emission rate with respect to the case of nano-emitters in a homogeneous medium (more precisely their emission rate will decrease). As nano-emitters, we have selected colloidal II-VI nanocrystals which are stable and present high quantum efficiency at room temperature. They are good candidates for single photon sources. For example, C. Vion et al. [39] showed an increase of the lifetime of about 10% for CdTeSe nanocrystals infiltrated in an opal made by sedimentation method compared with these nanocrystals in a homogeneous medium with the same refractive index (Figure 3). A way to obtain larger effects is to use inverted opals as they present high refractive contrast and complete photonic bandgap [18, 31, 25]. As an example, lifetime reductions up to 30% have been measured for CdSe Qdots infiltrated in titanium oxide inverted opals [16]. But the production of good quality inverted opals over large scale is not yet totally mastered.

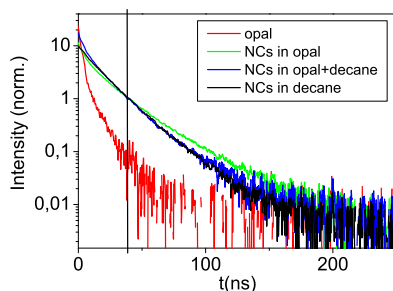


Figure 3: Luminescence Decay of Nanocrystals Embedded in an Opal (green line), Dissolved in Decane (black line), in the Opal Infiltrated with Decane (blue line). Self-luminescence of the Opal (red line).

3. Planar defect

The behaviour of nano-emitters in photonic crystals is somehow well understood. To go further in controlling the light emission and modifying the decay rate of nano-emitters, one has to introduce defects in the photonic structure. A controlled defect in the structure will disrupt the periodicity and create a cavity in which the emission will be confined

and the electromagnetic field enhanced as the local density of states. This defect can be obtained through the omission or the displacement of one or more holes in the case of planar photonic crystals for which the periodic variation of the dielectric constant is provided by drilling holes of a few hundred nanometers in diameter in a semiconductor matrix. For 3D-photonic crystals, a planar defect can be obtained. In this case, thanks to the defect, emission in preferred directions (creation of a pass-band inside the bandgap) and enhancement of the spontaneous emission rate should be observed. An interesting feature of 3D-photonic crystals is the potential ability to control light propagation in the three directions in space. One can expect to provide resonant coupling in one direction (the one on which the periodicity has been disrupted by the planar defect) as well as wave-guiding in the two other directions.

To engineer planar defects into colloidal PCs different bottom-up routes have been proposed by different groups. Planar defects have been fabricated by combining convective colloidal self-assembly and chemical vapour deposition to introduce a silica thin layer between two opal PCs [27, 37]. While these defects are passive, the Ozin group has also proposed active and tunable planar defects by incorporating polyelectrolyte multilayers having refractive index and thickness tuned by exposure to different solvent vapour pressures [36], UV-exposure as well as temperature. In this latter case, they obtain a full reversibility [11]. Another way to introduce a planar defect has been proposed by incorporating a monolayer of microspheres prepared by the Langmuir-Blodgett technique between two opal films with spheres of different diameters prepared by convective self-assembly. The LB technique supplies a well-defined single layer whereas it is difficult to realize such objective by using other self-assembly methods [43, 42].

We have selected two efficient and reliable methods to engineer a defect between two silica opals: by the transfer of a monolayer of silica spheres of different diameter by the Langmuir-Blodgett and Langmuir-Schaefer techniques or by sputtering a controlled amount of silica. The first one consists in the transfer of a compact monolayer composed with functionalized spheres of diameter larger than the one of the opal by the Langmuir-Blodgett (vertical transfer) or the Langmuir-Schaefer (horizontal transfer) techniques (Figure 4). If the first one is widely used to create opals layer by layer, the second one is usually devoted to transfer monolayers of small particles (gold nanoparticles or nano-emitters for example) and is rarely used for particles of this size. After the synthesis of a second opal on the transferred monolayer, the final structure was characterized by specular reflection spectroscopy. For both methods, a close to zero minimum of reflection, evidence of the defect mode, appeared in the stop-band. These results will be discussed on samples prepared by the second method. On Figure 5 one can see the good arrangement of the silica spheres of the sample.

The second method developed to create the defect layer consists in sputtering a certain amount of silica on the first opal. The sputtering conditions were chosen to grow the sputtered silica in a columnar way on the top of the spheres. Therefore, the obtained defect layer is made of elongated beads which keep very well the periodicity in the plane of the first opal and so permit a very well-ordered deposition of the second one. The structural quality is evidenced through SEM images of the edge of the sandwich structure (Figure 6).

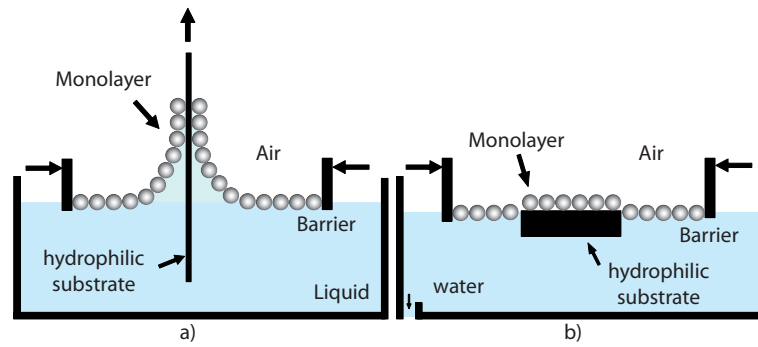


Figure 4: Langmuir Blodgett (a) and Langmuir Schaefer (b) Techniques.

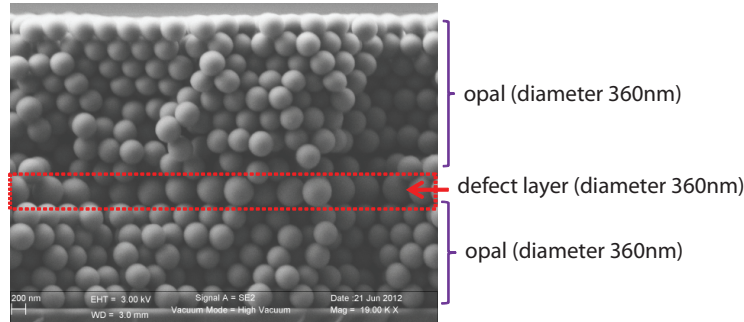


Figure 5: SEM Image of the Edge of the Sample with a Planar Defect Made by the LB Technique.

Several sandwich structures were prepared with different sputtered silica thicknesses. For a 123 nm-sputtered silica layer, the specular reflection spectra were performed for specular angles between 20° and 50° by step of 5° . Figure 7a shows the reflection spectra for 20° and 35° incidence angles. It appeared that, thanks to the defect, a pass-band was created in the stop-band. The spectral width of the pass-band was of the order of 25 nm. The value of the reflection minimum was almost zero. The corresponding contrast between reflected and transmitted optical modes, on the order of 90%, is very high compared to the best results reported in the literature. The spectral positions of the reflection minima for different incidence angles are plotted on Figure 7b (circles). The two extreme curves on Figure 7b correspond to the limits of the stop band taken to be the wavelengths closest to the maximum for which the reflection goes to zero on each side (see arrows on Figure 7 for 20° angle). By varying the angle from 20° to 50° , the defect mode spectral position goes from 717 nm to 598 nm, leading to a high tunability of almost 120 nm. Consequently, this kind of sandwich structure should be very suitable to allow wavelength-selective excitation and so to address selectively different emitters.

Finite Difference Time Domain (FDTD) Calculations

The experimental reflection and transmission spectra were compared with FDTD simulations using MEEP tool [26]. This method consists in calculating the propagation of the electromagnetic field from a given light source through a computed structure from the

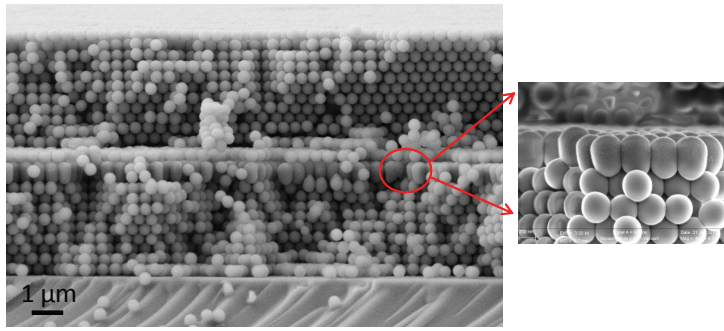


Figure 6: SEM Image of the Sandwich Structure.

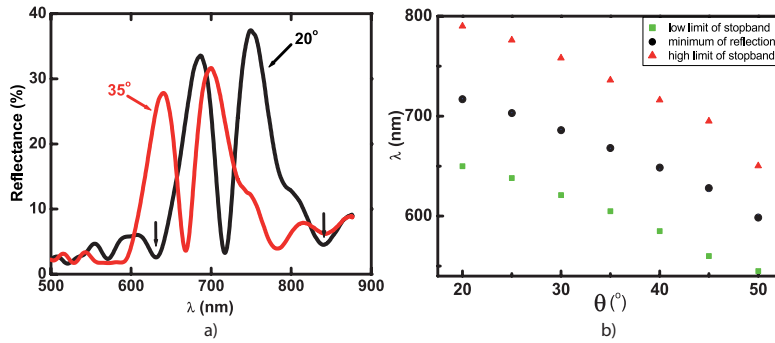


Figure 7: a) Experimental Reflection Spectra of the 123 nm-Defect Thickness Sample for 20° (black line) and 35° (red line) Incidence Angles. b) Position of the Reflexion Minima Versus the Incidence Angles (circles). The Triangles Correspond to the Limit of the Stop Band for High Wavelengths, the Squares to the Limit of the Stop Band for Low Wavelengths, Both Deduced from the Experimental Spectra.

Maxwell equations. For this, space and time are divided into a regular grid. The basic mechanism of this method is to discretize Maxwell's equations and to solve them in the leapfrog manner: the electric field vector components in a volume of space are solved at a given in time; then the magnetic field vector components in the same spatial volume are solved at a given time further; and the process is repeated until the desired transient or steady-state electromagnetic field behaviour is fully evolved.

The 0° -transmission spectra of the samples were simulated and compared with the experimental ones. For the 123 nm- thickness sample, a very good agreement was obtained (Figure 8) for the position of the defect mode, emphasizing the fact that the computed structure, simulated without any fitting parameter, is relevant. The position of the defect mode for various thicknesses of sputtered silica - 41, 87, 123 and 273 nm - was studied. The corresponding transmission spectra were measured and the simulations performed. Simulations were also run for other thicknesses between 150 and 450 nm. The results were summarized on Figure 9 which gives the spectral position of the defect mode versus the sputtered silica thickness. By controlling the amount of sputtered silica, one can monitor the position of the defect mode from the edge to the middle of the stop band.

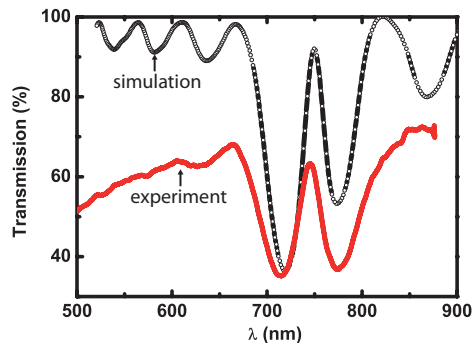


Figure 8: Experimental (red line) and Calculated (black line) 0° -Transmission Spectra of 123 nm-Defect Thickness Sample.

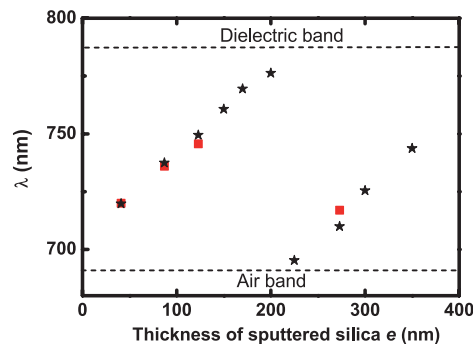


Figure 9: Maximum Wavelength of the Defect Mode for Different Thicknesses of Sputtered Silica: Simulations (star black point), Measurements (rectangle red point). The Dashed Horizontal Lines Correspond to the Edges of the Stopband Determined from the Experimental Spectra.

4. Modification of spectra and emission diagrams of CdTeSe nanocrystals

The prepared opal samples with a sputtered layer defect exhibit a pass-band around 700 nm for 20° . Therefore, CdSeTe nanocrystals which emit a band round 705 nm with a width of the order of 70 nm (Invitrogen Qdot 705 ITK) were selected. To introduce these nanoemitters in the defect layer, the procedure was the following: a drop of nanocrystals was deposited on the surface of the first opal covered by the sputtered silica (123 nm thick). Then, in order to protect these nanocrystals, a PMMA film (Polymethyl Methacrylate) was spin coated and then a heat treatment at 150°C was performed. Finally, the second opal was fabricated.

In order to control the quality of the photonic crystal after these procedures, the specular reflection spectra at the incidence angle of 20° of the samples with and without the nanocrystals and PMMA are compared on Figure 10. If the position of the defect mode is the same for both cases, unfortunately the defect mode is not as deep with the nano-emitters as with just the defect layer. That is a problem we will have to solve in the future. The nanocrystals were excited by a cw laser diode at a wavelength of 473 nm and the photoluminescence spectra were recorded for different detection angles by step of 2.5° .

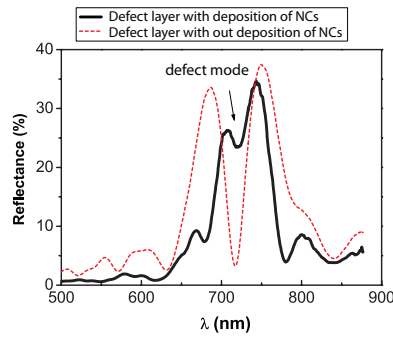


Figure 10: Reflection Spectra of the Sandwich Structure with the Defect Thickness of 123 m in the Cases of Samples with and without NCs.

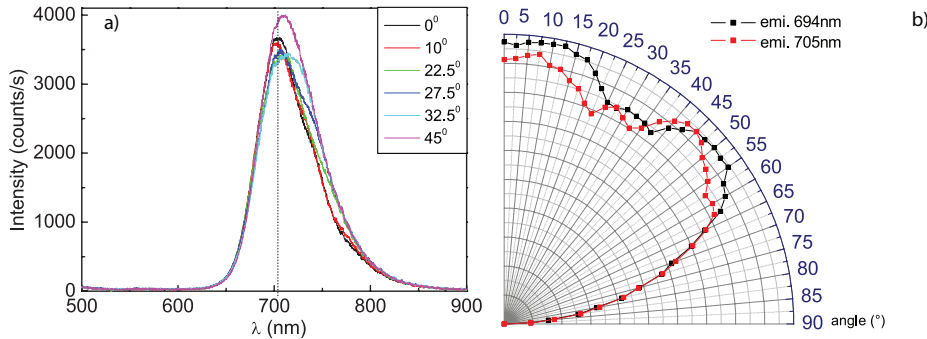


Figure 11: a) Luminescence Spectra of NCs Embedded in the Planar Defect of the Sandwich Structure with the Defect Thickness of 123 m. b) Diagrams of Radiation in Polar Representation at Two Different Wavelengths.

Depending on the collection angle, the maximum wavelength of the emission spectrum is shifted from 705 nm to 715 nm for incidence angles from 10° to 32.5° . Besides, the intensity of the emission spectra also varied (Figure 11a). The radiation diagrams are plotted as a function of the detector angle at wavelengths of 705 and 694 nm (Figure 11b). One can see a decrease of the intensity of the emission in the angle range 25° - 45° with a small increase around 30° and 35° . That corresponds to the stop-band and the pass-band localizations for these angles. In addition, the lambertian emission is kept for angles higher than 65° for which the stop band is completely out of the emission band of the nanoemitters. These results can be discussed just by considering the filter effect of the opal with a planar defect. The analysis of the emission decay modification is necessary to evidence the action of the photonic crystals on the emission of the nanocrystals.

5. Conclusion

Artificial opals with a planar defect can be considered as a good "model system" to study the modification of the optical properties of nanoemitters in a photonic crystal. We have prepared silica opals by the convective method and introduced in the middle of the opal a planar defect by the Langmuir techniques or by sputtering some amount of silica. This defect opens a pass-band in the stop-band of the photonic crystal. Nanocrystals

for which the emission band is located in the stop-band of the opal were embedded in the defect layer. The collected fluorescence of these nanocrystals presents an emission diagram which is modified by the photonic crystal and especially by the defect layer. Preliminary experiments on the fluorescence of nanocrystals embedded in an opal showed that it is possible to record the emission decay of a single nanoemitter. This is the first step towards the study of the photonic environment on a single photon emitted by a single nanocrystal embedded within the opal defect layer.

References

- [1] V.N. Astratov, Yu.A. Vlasov, O.Z. Karimov, A.A. Kaplyanskii, YU.G. Musikhin, N.A. Bert, V.N. Bogomolov, and A.V. Prokofiev. *Physics Letters A*, 222:349, 1996.
- [2] A. Avoine, P. Hong, H. Frederich, J.-M.Frigerio, L. Coolen, C. Schwob, Pham Thu Nga, B. Gallas, and A. Maitre. *Phys. Rev. B*, 86:1, 2012.
- [3] A. V. Baryshev, A. A. Kaplyanskii, V. A. Kosobukin, M. F. Limonov, K. B. Samusev, and D. E. Usvyat. *Phys. Sol. State*, 45:459, 2003.
- [4] A. V. Baryshev, A. A. Kaplyanskii, V. A. Kosobukin, M. F. Limonov, and A. P. Skvortsov. *Phys. Sol. State*, 46:1331, 2004.
- [5] A. V. Baryshev, A.B. Khanikaev, R. Fujikawa, H. Uchida, and M. Inoue. *Phys. Rev. B*, 76:014305, 2007.
- [6] A. G. Bazhenova, A. V. Sel'kin, A. Yu. Men'shikova, and N. N. Shevchenko. *Phys. Sol. State*, 49:2109, 2007.
- [7] P.V. Braun, R.W. Zehner, C.A. White, M.K. Weldon, C. Kloc, S.S. Patel, and P. Wiltzius. *Advanced Materials*, 13:721, 2001.
- [8] M. Campbell, D.N. Sharp, M. T. Harrison, R.G. Denning, and A.J. Turberfield. *Nature*, 404:53, 2000.
- [9] M. Deubel, G. Von Freymann, M. Wegener, S. Pereira, K. Bush, and C. M. Soukoulis. *Nature Materials*, 3:444, 2004.
- [10] I. Divliansky, T.S. Mayer, K. S. Holiday, and V. Crespi. *Applied Physics Letters*, 82:1667, 2003.
- [11] F. Fleischhaker, A. C. Arsenault, V. Kitaev, F.C. Peiris, G. von Freymann, I. Manners, R. Zentel, and G.A. Ozin. *J. Am. Chem. Soc.*, 127:9318, 2005.
- [12] J.G. Fleming and Shawn-Yu Lin. *Optics letters*, 24:49, 1999.
- [13] J. F. Galisteo-Lopez, F. Lopez-Tejeira, S. Rubio, C. Lopez, and J. Sanchez-Dehesa. *Appl. Phys. Lett.*, 82:4068, 2003.

- [14] P. Jiang, J.F. Bertone, K.S. Hwang, and V.L. Colvin. *Chemical Materials*, 11:2132, 1999.
- [15] Ngoc Diep Lai, Wen Ping Liang, Jian Hung Lin, Chia Chen Hsu, and Cheng Hsiung Lin. *Optics Express*, 13:9605, 2005.
- [16] P. Lodahl, F. van Driel, I. S. Nikolaev, A. Irman, K. Overgaag, D. Vanmaekelbergh, and W. L. Vos. *Nature*, 430:654, 2004.
- [17] F. Lopez-Tejiera, T. Ochiai, K. Sakoda, and J. Sanchez-Dehesa. *Phys. Rev. B*, 65:195110, 2002.
- [18] M. Megens, J.E.G. Wijnhoven, A. Lagendijk, and W.L. Vos. *Phys. Rev. A*, 59:4727, 1999.
- [19] H. Miguez, C. Lopez, F. Meseguer, A. Blanco, L. Vasquez, R. Mayoral, M. Ocana, V. Fornes, and A. Mifsud. *Applied Physics Letters*, 71:1148, 1997.
- [20] H. Miguez, F. Meseguer, C. Lopez, A. Mifsud, J.S. Moya, and L. Vasquez. *Langmuir*, 13:6009, 1997.
- [21] Y. V. Miklyaev, D.C. Meisel, A. Blanco, G. von Freymann, K. Bush, W. Koch, C. Enkrich, M. Deubel, and M. Wegener. *Applied Physics Letters*, 82:1284, 2003.
- [22] V. Mizeikis, K. Khuen Seet, S. Juodkazis, and H. Mizawa. *Optics Letters*, 29:2061, 2004.
- [23] A. V. Moroz, M. F. Limonov, M. V. Rybin, and K. B. Samusev. *Phys. Sol. State*, 53:1105, 2011.
- [24] R. V. Nair and B. N. Jagatap. *Phys. Rev. A*, 85:013829, 2012.
- [25] I.S. Nikolaev, P. Lodahl, A.F. van Driel, A.F. Koenderink, and W.L. Vos. *Phys. Rev. B*, 75:115302, 2007.
- [26] A. F. Oskooi, D. Roundy, M. Ibanescu, P. Bermel, J. D. Joannopoulos, and S. G. Johnson. *Computer Physics Communications*, 181:687, 2010.
- [27] E. Palacios-Lidon, J. F. Galisteo-Lopez, B. H. Juarez, and C. Lopez. *Advanced Materials*, 16:341, 2004.
- [28] A. Quattieri, G. Morello, P. Spinicelli, M. Todaro, T. Stomeo, L. Martiradonna, M. De Giorgi, X. Quelin, S. Buil, A. Bramati, J-P. Hermier, R. Cingolani, and M. De Vittorio. *New Journal of Physics*, 11:033025, 2009.
- [29] S. Reculosa and S. Ravaine. *Chem. Mater*, 15:598, 2003.
- [30] S. G. Romanov, T. Maka, C. M. Sotomayor Torres, M. Muller, R. Zentel, D. Cassagne, J. Manzanares-Martinez, and C. Jouanin. *Phys. Rev. E*, 63:056603, 2001.

- [31] V. Solovyev. *Journal of Applied Physics*, 94:1205, 2003.
- [32] W. Stober, A. Fink, and E. Bohn. *J. of Colloid and Interface Science*, 69:62, 1968.
- [33] H. B Sun, S. Matsuo, and H. Misawa. *Applied Physics Letters*, 74:786, 1999.
- [34] M. Szekeres, O. Kamalin, R.A. Schoonheydt, K. Wostyn, K. Clays, A. Persoons, and I. Dekany. *J. of Mater. Chem.*, 12:3268, 2002.
- [35] A. Tikhonov, J. Bohn, and S. A. Asher. *Phys. Rev. B*, 80:235125, 2009.
- [36] N. Tretreault, A.C. Arsenault, A. Mihi, S. Wong, V. Kitaev, I. Manners, H. Miguez, and G.A. Ozin. *Advanced Materials*, 17:1912, 2005.
- [37] N. Tretreault, A. Mihi, H. Miguez, I. Rodriguez, G.A. Ozin, F. Meseguer, and V. Kitaev. *Advanced Materials*, 16:346, 2004.
- [38] H. M. van Driel and W. L. Vos. *Phys. Rev. B*, 62:9872, 2000.
- [39] C. Vion, C. Barthou, P. Benalloul, C. Schwob, L. Coolen, A. Gruzintev, G. Emelachenko, W. Masalov, J.-M. Frigerio, and A. Maitre. *J. Appl. Phys.*, 105:113120, 2009.
- [40] Y. A. Vlasov, Xiang-Zheng Bo, J.C. Sturm, and D. J. Norris. *Nature*, 414:289, 2001.
- [41] S. Wong, V. Kitaev, and G.A. Ozin. *J. Am. Chem. Soc.*, 125:15589, 2003.
- [42] K. Wostyn, Y. Zhao, G. de Schaetzen, L. Hellemans, N. Matsuda, K. Clays, and A. Persoons. *Langmuir*, 19:4465, 2003.
- [43] Y. Zhao, K. Wostyn, G. de Schaetzen, K. Clays, L. Hellemans, A. Persoons, M. Szekeres, and R.A. Schoonheydt. *Applied Physics Letters*, 82:3764, 2003.

Paul Benalloul
Institut des NanoSciences de Paris, 75005 Paris, France
E-mail: paul.benalloul@insp.jussieu.fr